Marek's disease virus-encoded miR-155 ortholog critical for the induction of lymphomas is not essential for the proliferation of transformed cell lines

Marek's disease virus-encoded miR-155 ortholog critical for the induction of lymphomas is not essential for the proliferation of transformed cell lines

Yaoyao Zhang[1, 2], Na Tang[1, 3], Jun Luo[4,5], Man Teng[4], Katy Moffat[1], Zhiqiang Shen[3], Mick Watson[6], Venugopal Nair[1,7,8#], Yongxiu Yao[1#]

[1]The Pirbright Institute & UK-China Centre of Excellence for Research on Avian Diseases, Pirbright, Guildford, Surrey, United Kingdom

[2]School of Animal Science and Technology, Guangxi University, Nanning, China

[3]Binzhou Animal Science and Veterinary Medicine Academy & UK-China Centre of Excellence for Research on Avian Diseases, Binzhou, China

[4]Key Laboratory of Animal Immunology of the Ministry of Agriculture, Henan Provincial Key Laboratory of Animal Immunology, Henan Academy of Agricultural Sciences, Zhengzhou, China

[5]College of Animal Science and Technology, Henan University of Science and Technology, Luoyang, China

[6]The Roslin Institute, R(D)SVS, University of Edinburgh, Easter Bush, Midlothian, UK

[7]The Jenner Institute Laboratories, University of Oxford, Oxford, United Kingdom

[8]Department of Zoology, University of Oxford, Oxford, United Kingdom

 # Corresponding Authors

E-mail: yongxiu. yao@pirbright.ac.uk & venugopal.nair@pirbright.ac.uk

Running title: MDV-miR-M4 not needed for maintaining transformation

Abstract

MicroRNAs (miRNAs) are small non-coding RNAs with profound regulatory roles in many areas of biology, including cancer. MicroRNA 155 (miR-155), one of the extensively studied multifunctional miRNAs, is important in several human malignancies such as diffuse large B cell lymphoma and chronic lymphocytic leukemia. Moreover, miR-155 orthologs KSHV-miR-K12-11 and MDV-miR-M4, encoded by Kaposi's sarcoma-associated herpesvirus (KSHV) and Marek's disease virus (MDV) respectively, are also involved in oncogenesis. In MDV-induced T-cell lymphomas and lymphoblastoid cell lines derived from them, MDV-miR-M4 is highly expressed. Using excellent disease models of infection in natural avian hosts, we showed previously that MDV-miR-M4 is critical for the induction of T-cell lymphomas as mutant viruses with precise deletions were significantly compromised in their oncogenicity. However, these studies did not elucidate whether continued expression of MDV-miR-M4 is essential for maintaining the transformed phenotype of tumor cells. Here using an *in situ* CRISPR/Cas9 editing approach, we deleted MDV-miR-M4 from the MDV-induced lymphoma-derived lymphoblastoid cell line MDCC-HP8. Precise deletion of MDV-miR-M4 was confirmed by PCR, sequencing, quantitative RT-PCR and functional analysis. Continued proliferation of the MDV-miR-M4-deleted cell lines demonstrated that MDV-miR-M4 expression is non-essential for maintaining the transformed phenotype, despite its initial critical role in the induction of lymphomas. Ability to examine the direct role of oncogenic miRNAs *in situ* in tumour cell lines is valuable in delineating distinct determinants and pathways associated with the induction or maintenance of

transformation in cancer cells and will also contribute significantly to gain further insights into the biology of oncogenic herpesviruses.

Journal of Virology JVI Journal of Virology

Importance

Marek's disease virus (MDV) is an alphaherpesvirus associated with Marek's disease, a highly contagious neoplastic disease of chickens. MD serves as an excellent model for studying virus-induced T-cell lymphomas in the natural chicken hosts. Among the limited set of genes associated with MD oncogenicity, MDV-miR-M4, a highly expressed viral ortholog of the oncogenic miR-155, has received extensive attention due to its direct role in the induction of lymphomas. Using a targeted CRISPR-Cas9-based gene editing approach in MDV-transformed lymphoblastoid cell lines, we show that MDV-miR-M4, despite its critical role in the induction of tumours, is not essential for maintaining the transformed phenotype and continuous proliferation. As far as we know, this is the first study where precise editing of an oncogenic miRNA has been carried out *in situ* in MD lymphoma-derived cell lines to demonstrate that it is not essential in maintaining the transformed phenotype.

Introduction

MicroRNAs (miRNAs) are ~22-nucleotide small RNA molecules that function as master regulators of gene expression in many species including plants, worms, flies, animals, as well as in a number of viruses. Most of the virus-encoded miRNAs are seen in DNA viruses, with members of the family Herpesviridae accounting for the vast majority demonstrating the significance of miRNA-mediated gene regulation in the biology of herpesvirus infection (1-3). Identification of miRNAs encoded by human oncogenic γ-herpesviruses such as Kaposi's sarcoma-associated herpesvirus (KSHV) and Epstein-Barr virus (EBV) as well as avian oncogenic α-herpesvirus Marek's disease virus (MDV) has highlighted the potential contribution of the virus-encoded miRNAs towards the oncogenicity of these viruses. Among the several roles of the herpesvirus-encoded miRNAs such as immune evasion, control of viral latency/lytic replication and oncogenic potential (4-6), the role of viral orthologs of host miR-155 encoded by KSHV and MDV in oncogenesis has been most extensively studied (5, 7). As a multifunctional miRNA expressed primarily in the hematopoietic and cells of the immune systems, miR-155 is highly conserved in most species including humans and chickens, and are associated with different lymphomas (8-11). In EBV-induced B-cell transformation as well as in a number of EBV-associated B-cell lymphomas including Hodgkin's lymphoma, diffuse large B-cell lymphoma (DLBCL) and Burkitt's lymphoma in humans, upregulation of miR-155 resulting in escalated cell proliferation and neoplastic transformation has been reported (12, 13). KSHV, a human gammaherpesvirus associated with lymphoproliferative disorders such as primary effusion lymphoma (PEL), multicentric Castleman disease (MCD) and B lymphomagenesis in AIDS patients, encodes 25

miRNAs. Among these miRNAs, KSHV-K12-11 that plays critical role in pathogenesis is a functional ortholog of hsa-miR-155 sharing identical seed sequences (14-16). MDV encodes MDV-miR-M4-5p (miR-M4), a functional ortholog with identical seed sequences with miR-155 and KSHV-K12-11 that has been shown to play a critical role in the induction of lymphomas (6).

Marek's disease (MD) is a lymphoproliferative disease of chickens characterized by rapid-onset lymphomas in multiple organs, and infiltration into peripheral nerves causing paralysis. MD serves as an excellent model for studying virus-induced T-cell lymphomas. Among the more than 100 genes encoded by the MDV (17, 18), the basic leucine zipper protein Meq (MDV *Eco*RI Q), which is expressed both in lytic and latent infections undisputedly, is the most important viral gene associated with MD oncogenicity (19, 20). Deleting the Meq gene or inhibition of its important interactions with host proteins such as c-Jun, c-Fos and C-terminal binding protein (CtBP) can affect the oncogenicity of the virus (21-23). Although the viral telomerase RNA (vTR) also has been shown to promote MDV-induced oncogenesis (24), the role of MDV-encoded miRNAs in oncogenesis has drawn extensive attention (25-27). MDV encodes 14 miRNA precursors producing 26 mature miRNAs which are clustered into three separate genomic loci within the repeat regions of the viral genome. MDV-miR-M4, located in the cluster 1, was shown to be the viral ortholog of miR-155 (28). The oncogenic property of miR-155 together with the observation of high level of miR-M4 expression in tumor cells and the identification of several cancer pathway-related target genes suggested the important role of this miRNA in MDV-induced oncogenesis. Indeed, we and others have previously demonstrated the direct role of miR-M4 in the induction of tumours using recombinant MDV engineered to

have deletion- or seed region- mutations in miR-M4 using *in vivo* experiments in chickens (6, 29). Furthermore, we showed that the loss of oncogenic phenotype of miR-M4-deletion mutant of MDV can be partially rescued by MDV expressing gga-miR-155 demonstrating the similarities in the function of the two orthologs (6). While the role of miR-M4 in the induction of MD lymphomas has been clearly demonstrated in these studies, it remains unclear whether continued high level expression of miR-M4 is essential for maintaining the transformed phenotype of MDV-transformed tumour cells. As clonal populations of transformed tumor cells with latent MDV genome and limited gene expression (30-32), lymphoblastoid cell lines (LCL) derived from MD lymphomas have served as valuable resources to understand distinct aspects of virus-host interactions in transformed cells. However detailed investigations into the role of different viral and host determinants in these cells have been difficult due to the lack of tools for manipulation of viral/host genomes of these cells *in situ*. Following our recent success in efficient editing of the MDV genome in cell culture systems *in vitro* that supports lytic virus replication (33), we explored the use of a gene editing approach in MDCC-HP8 cell line that is latently infected with GA strain of MDV. Using MDCC-HP8 cells that stably expressed Cas9 and synthetic gRNAs with two-part guide RNA system, we examined the effect of deleting miR-M4 to gain insights into its functional role. Continued proliferation of the miR-M4 knock-out cell lines suggested that expression of miR-M4 gene is not essential for maintenance of the transformed state of the tumor cell line MDCC-HP8, despite its known critical role in the induction of MD lymphomas

Results

Knockout of MDV-miR-M4 in HP8 cells

Based on the success of efficient editing of the MDV genome during lytic replication in infected chicken embryo fibroblast (CEF) cultures in our previous studies (33), we attempted editing of the latent MDV genome in virus-transformed cell lines. Initial attempt with transfected gRNA-Cas9-expression plasmid showed low editing efficiency, thought to be largely due to the relatively low transfection efficiency of the hard-to-transfect MDV-transformed cell lines (data not shown). New gene editing strategy involving the transfection of synthetic gRNAs with two-part guide RNA system into MDV-transformed cell line stably expressing Cas9 (HP8-Cas9) showed great success. For the targeted editing of the MDV-miR-M4 in the latent viral genome in this cell line, two gRNAs M4-gN and M4-gC were designed using CRISPR guide RNA designing software (http://crispr.mit.edu/). M4-gN targeted the upstream sequence of the mature miR-M4 sequence and M4-gC targeted the sequence spanning the mature miR-M4 sequence and the loop region of the pre-miRNA hairpin structure resulting in the predicated cleavage site exactly lies at the end of the miR-M4 mature sequence (Fig. 1a & 1b). Successful miR-M4 deletion would release a 54-nt fragment following the successful cleavage of the sequence by the two gRNAs. Considering the presence of several MDV genomes integrated in multiple chromosomes of the chicken genome based on fluorescence *in situ* hybridization (FISH) analysis (unpublished data) and the location of miR-M4 in the terminal repeat region which doubles the copy number of miR-M4, two distinct bands are expected with PCR tests on the genomic DNA from cells harvested 48 h after transfection using specific primers located at the flanking region of Cas9 targeting sites. The top band of around 205-bp represented the unedited sequence or edited target site/s with small indels if the two sites are not cleaved simultaneously. The bottom

smaller band of around 151-bp product corresponded to the edited region with 54bp deletion between the two Cas9 cleavage sites. Interestingly, only the bottom band was detected by PCR analysis indicating the highly efficient cleavage with the two gRNAs with the majority of the cells transfected and edited efficiently. Despite of observation of single band, single cell sorting was carried out to obtain pure population of miR-M4 deleted cell. Although only bottom band was obtained by PCR before sorting in the mixed population, clones with top band were predominant after single cell cloning (Fig. 1c). Sequence analysis of four bottom bands confirmed that it represented the direct end joining product of two predicted Cas9 target sites (Fig. 1a). Interestingly, the sequences of all these four clones were identical suggesting that further screening of several additional clones may be required to identify variations within the edited sequences. The successful knockout of miR-M4 sequence was further confirmed by qRT-PCR analysis, using uninfected CEF as a negative control. As expected, miR-M4 was absent from all four miR-M4-deleted HP8 clones and control CEF, compared to the high level expression detected in the parental HP8-Cas9 cells (Fig. 1d). These experiments demonstrated that miR-M4 has been deleted successfully with two-part guide RNA system in HP8 cell line stably expressing Cas9.

miR-M4 is not essential in maintaining the transformed phenotype of MDV-transformed cell line

miR-M4 has been shown to be essential for the MDV in inducing tumors (6, 29). To explore the role of miR-M4 in maintaining the transformed state, we examined the effect of deletion of miR-M4 on the proliferation of HP8 cells. For this, we carried out kinetic monitoring of proliferation of the wild type HP8-Cas9 and the miR-M4 deleted clones

using IncuCyte S3 Live-Cell Imaging system. The cell proliferation data in real time from the images collected at 4 hours intervals showed that the miR-M4-deleted clones proliferated at a significantly higher rate within the first three days compared to parental HP8-Cas9 cells although different clones showed different levels of significance at various time points. These results suggested that expression of miR-M4 was not essential for the proliferation phenotype of these transformed cells.

Pu.1 is up-regulated in HP8-ΔmiR-M4 cells

Having shown that miR-M4 can be deleted from HP8 cell line and that it is not essential for the continued proliferation of these transformed cells, we wanted to examine the effect of miR-M4 deletion on the expression of its target proteins. For this, we chose to analyze the expression levels of Pu.1, one of the very well characterised and validated miR-M4 target (28). This was first assessed using luciferase reporter assay by transfection of the reporter construct containing the wild-type predicted miR-M4-response element (MRE) or the mutant MRE region of the 3′ UTR of Pu.1 into the miR-M4-deleted and the parental HP8-Cas9 cells. This assay showed that the relative Renilla luciferase levels of reporter constructs with wild-type MRE sequences were reduced by nearly 40% compared with the mutant MRE construct in the parental HP8-Cas9 cells. Compared to this, such reduction of luciferase levels was absent in all of the miR-M4 deleted clones (Fig. 3a) demonstrating the functional effect of miR-M4 deletion on the Pu.1 target. Next, we determined the miR-M4-mediated silencing by directly measuring the level of Pu.1 expression in one of the selected mutant clones C48, along with the parental cells. Immunoprecipitation-Western blot analysis showed that Pu.1 expression level was much higher in miR-M4-deleted cells compared with the parental cells (Fig.

3b). Results from the reporter assay and the direct expression analysis of the Pu.1 target have thus confirmed the deletion and functional consequences of miR-M4 in the mutant C48 clone.

Effect of miR-M4 deletion on expression of other viral miRNAs and Meq protein

Having demonstrated successful knockout of miR-M4 from MDV genome in HP8 cell line, we next analyzed the effect of miR-M4 deletion on expression of other MDV-encoded miRNAs and the major viral oncoprotein Meq. The 14 MDV-encoded miRNA precursors are clustered into three separate genomic loci. Cluster 1 (Meq cluster) containing miR-M2, 3, 4, 5, 9 and 12 located upstream of Meq gene. The mid-cluster containing three miRNA precursors (miR-M11, 31 and 1) located downstream of Meq. The third cluster, referred to LAT-cluster, lies within the first intron of latency-associated transcript (LAT). To assess the potential effect of miR-M4 deletion on other miRNAs, we first amplified the cluster 1 miRNAs by PCR with the primers at the flanking region of the cluster. Sequence of the PCR product was determined to confirm the absence of any changes (data not shown) except for the edited region as shown in Figure 1a. Next we analysed the expression of each miRNA in cluster 1, miR-M31 from cluster 2, miR-M6 and miR-M8 from cluster 3 using the RNA extracted from miR-M4-deleted clone 48 and the parental HP8-Cas9. The host miRNA gga-let-7a was also measured, with total RNA from uninfected CEF used as control. As shown in Figure 4a, all viral miRNAs were absent and only let-7a was detectable in the CEF sample. Except for the absence of miR-M4 from miR-M4-deleted clone 48, both the viral and the host miRNAs were detected in HP8 before or after miR-M4 deletion. Quantitation of selected viral miRNAs by qRT-PCR indicated that they are still expressed in the miR-M4-deleted clone 48, although

their expression levels showed variation compared to the parental HP8 cells (Fig. 4a). We also examined Meq expression in the miR-M4-deleted cells by western blot analysis. An ALV-transformed B-cell line HP45 and uninfected CEF which do not express Meq were used as negative controls. Results of the western blot analysis confirmed the expression of Meq in the miR-M4-deleted cells, demonstrating that miR-M4 was not required for Meq expression in these cells (Fig. 4b).

v-*rel* relieves the inhibition of miR-155 expression in HP8-ΔmiR-M4

We have previously shown that miR-155 is consistently downregulated in MDV-transformed tumours and cell lines (34) and this downregulation can be rescued by expressing v-*rel* that also activate the expression levels of miR-M4 in these cells (35). We wanted to examine whether the downregulation of miR-155 can be rescued without the activation of miR-M4 by transduction of v-*rel* with RCAS(A)-v-*rel*-GFP virus in HP8-ΔmiR-M4 clone 48. The GFP marker allowed sorting of the RCAS-infected cells. Analysis of the sorted cells by Western blotting confirmed the expression of v-*rel*-GFP in RCAS(A)-v-*rel*-GFP-infected cells and GFP expression in RCAS(A)-GFP infected cells (Fig. 5a). Expression of v-*rel* increased the level of miR-155 expression by approximately 6026-fold in HP8-ΔmiR-M4 cells but only 25-fold in HP8-Cas8 cells (Fig. 5b), demonstrating that deletion of miR-M4 increased miR-155 expression induced by v-*rel*.

Discussion

Virus-host interactions in herpesviruses are characterized by long term survival as latent infections in different cell types. With total dependence on the host cell, several viruses have adopted strategies to modulate the host cellular environment, including the

249 modulation of miRNAs. A number of studies have demonstrated the role of miRNAs in
250 replication, pathogenesis and oncogenesis of herpesviruses (3, 4, 7, 36-38). These
251 included our own studies demonstrating the critical role of miR-M4 in the induction of
252 lymphomas by MDV (6). While these observations have also been confirmed by other
253 studies (29), the role of viral miRNAs in maintaining the transformed state, as well as in
254 other functions such as the switch of latency/lytic replication in tumor cells have not been
255 examined. Particularly, the role of miR-M4, the viral ortholog of oncogenic miR-155
256 encoded by oncogenic MDV, in maintaining the transformed phenotype of the tumor cell
257 line is unknown. MDV-transformed LCLs derived from MD lymphomas which contain
258 multiple copies of MDV genome integrated in different chromosomes are valuable to
259 study latency, transformation and reactivation *in situ*. Having established the
260 CRISPR/Cas9-based editing of the viral genome at relatively high efficiency in MDV-
261 transformed cell lines, we report here the precise knockout of miR-M4 from the MDV
262 genome in the LCL HP8. Results from these studies show that miR-M4, despite its
263 critical role in the induction of lymphomas by oncogenic MDV strains, is not required for
264 the continued proliferation of MDV-transformed HP8 LCL. As far as we know, this is the
265 first study that makes use of the CRISPR/Cas9-based gene editing technology *in situ* to
266 demonstrate that a critical virus-encoded miRNA is not essential to maintain the
267 transformed phenotype of a virus-induced cancer cell line.

268 By transfection of two parts synthetic gRNA into HP8 cells stably expressing Cas9, we
269 have shown here that miR-M4 can be deleted at a relatively high efficiency (Fig. 1c).
270 Considering the presence of the multiple copies of the target loci in these cell lines, the
271 high editing efficiency highlighted that efficient gRNA, rather than the copy numbers of

the target genes, is the key to achieve the desired editing even in the hard-to-transfect cell lines such as the MDV-transformed LCL. Although the editing efficiency based on the PCR test on the transfected cell lines appeared to be very high, sorting of the single cell populations did identify a number of unedited clones, further highlighting the importance of single cell sorting in gene editing pipelines. These findings are also consistent with our observation that the recovery rate of edited cells is probably much lower than that of the unedited cell populations, suggesting that single cell cloning is a required step to get the pure populations of the edited cells regardless of the efficiency of gene editing. The successful knockout of miR-M4 demonstrated the value of this approach in identifying other molecular determinants associated with different phenotypes including latency/lytic switch in LCLs. While the growth of the miR-M4-deleted cells confirmed that the expression of miR-M4 is not essential to maintain the transformation and proliferation of LCL, ΔmiR-M4 cell line that we have generated will also be a valuable research tool for addressing significant biological questions in the future on the functional role of this important miRNA homolog. For example, it will be interesting to know if the populations of shared target genes of MDV-miR-M4, miR-155 and KSHV-miR-K12-11 (5) are upregulated in the miR-M4-deleted cells and downregulated after v-*rel* transduction which activates miR-155 expression (Fig. 5b). Similarly, future studies on the global analysis of the changes in the transcriptome and proteomes of the edited cell populations, together with changes in the viral and host epigenomes will throw more insights into the fine tuning of the molecular regulatory network around these family of miRNAs in these virus-transformed cell lines. Finally, these cells also give the opportunity to investigate

the role of miR-M4 to induce lymphomas (transplantable tumors) *in vivo* in experimentally-infected target chicken hosts.

Repair by non-homologous end joining (NHEJ) is usually accompanied by random nucleotide insertion/deletion at cleavage site. As a result, the edited sequence is most likely to be a mixed population. However, sequencing results have shown that virtually all of edited sequences are end joining product of the two predicted Cas9 cleavage sites. Although additional variations may be discovered when more clones are analyzed, the edited loci often contained only predominant mutant sequence as we have shown previously (33, 39). The reasons for the clonal nature of the appearance of the single population are not fully clear. Whether this is related to the stable expression of the Cas9 in these cells or due to other factors require further investigation.

The oncogene v-*rel* activates miR-155 expression by binding to NF-κB site in Bic promoter. We have shown previously that the downregulation of miR-155 in MDV-transformed cell lines could be rescued by expressing v-*rel* in these cells (35). Using the same approach, we have shown here that the downregulation of miR-155 can also be rescued in the context of miR-M4 deleted HP8 by transduction of v-*rel* with RCAS(A)-v-*rel*-GFP virus in HP8-ΔmiR-M4 clone C48. Interestingly, only 25-fold increase of miR-155 level could be induced in the unedited HP8-Cas9 cells compared to 6,026-fold increase in the miR-M4 deleted clone C48, suggesting that the absence of miR-M4 significantly enhances the ability of v-*rel* to induce miR-155 expression in MDV tumor cell lines. As has been demonstrated previously, miR-M4 is highly expressed in MDV tumor cell lines compared to the miR-155, which is actively downregulated, although the precise mechanisms of the differential downregulation have not been identified. Based on

the findings from the present study, it appears that the downregulation of miR-155 may be directly linked to high level of miR-M4 expression as the activation of miR-155 by v-*rel* is more robust in the miR-M4-deleted cells. However, further studies are required to delineate the associated mechanisms involved in such regulation.

The precise editing of the miR-M4 locus to abolish the expression of the mature miR-M4 in the MDV-induced T-lymphoma-derived cell line HP8, clearly demonstrated that the proliferative capacity of the transformed cell line is not dependent on continued high level expression of miR-M4. The continued proliferation of cells is unlikely to be due to the inability to express other viral miRNAs such as all other miRNAs in cluster 1 and selected miRNAs from both mid-cluster and LAT-cluster detected by miRNA qRT-PCR (Fig. 4a). MDV-miR-M4 is very important for the oncogenicity of MDV but other miRNAs in the cluster also contribute since the mutant virus expressing miR-M4 alone in cluster 1 remained non-oncogenic (6). Whether or not other miRNA contribute to the maintenance of transformed phenotype remains to be elucidated. The continued proliferation of cells is also not due to the lack of expression of adjacent viral gene such as Meq as we were able to demonstrate the expression of the protein by western blot analysis (Fig. 4b). The significantly increased proliferation capacity of miR-M4 knockout clones suggests that miR-M4 in these context may have proliferation suppressor function. Additional studies on the detailed analysis of the gene expression profiles on these clones will be required to gain further insights into the biology of miR-M4 in these cells. Although it is possible that LCLs may have acquired other mutations that may have made them no longer dependent on miR-M4 for proliferation, the failure on rescuing Meq deleted cell line after repeated attempts indicated this is unlikely the case. Whether or not

other genes or miRNAs are involved in maintaining the transformed phenotype of MD tumor cell lines remains to be investigated.

Materials and Methods

Cell Culture

The MDV-transformed lymphoblastoid cell lines HP8 (40) from a GA strain-induced tumour were grown at 38.5°C in 5% CO_2 in RPMI 1640 medium (Life technologies) containing 10% fetal bovine serum, 10% tryptose phosphate broth, 1% sodium pyruvate solution (Sigma) and 100 units/mL of penicillin and streptomycin (Life technologies).

gRNAs

Two-part guide RNA system containing crRNA:tracrRNA guide complex was used for editing. The sequences of gRNA miR-M4-gN and miR-M4-gC listed in Table 1 were used for synthetic crRNAs production by Integrated DNA Technologies (IDT, USA). The tracrRNA was purchased from IDT. The lyophilized crRNA and tracrRNA pellets were resuspended in Duplex buffer (IDT) at 200 µM concentration and stored in small aliquots at −80°C.

Generation and characterization of HP8-ΔmiR-M4 cell line

NEPA21 Electroporator was used for the transfection of HP8 cells that stably expressed Cas9 (HP8-Cas9) (41). For the deletion of miR-M4, $1x10^6$ of HP8-Cas9 cells were resuspended in 96µL Opti-MEM medium. Two crRNAs miR-M4-gN and miR-M4-gC were mixed with equal molar amounts of tracrRNA to a final duplex concentration of 100 µM in 4 µL of duplex buffer and incubated at 95°C for 5 min. After the duplex was allowed to cool to room temperature, it was mixed with cell suspension and electroporated using the conditions of voltage 275V and pulse width 1.5ms of poring

Journal of Virology

pulse. At 48 h post electroporation, $1x10^5$ cells were harvested and analysed by PCR. The remaining cells were sorted into 96 wells for single cell isolation. After 7 days incubation, cells were collected and analyzed by PCR. The harvested cell for PCR analysis were lysed in 1× protein K based DNA isolation buffer (33) at 65 °C for 30 min. 1 µL of extracted DNA template was used for PCR with primers outside the targeted sites to identify the correct miR-M4 gene knock-out. The primer sequences of miR-M4-F and miR-M4-R used for PCR are listed in Table 1.

RCAS virus infection

Virus stocks were generated from DF-1 cells transfected with RCAS(A)-EGFP and RCAS(A)-v-*rel*-EGFP constructs approximately 5 days after transfection, when 100% cells were EGFP-positive. For v-*rel* transduction in HP8-Cas9 and HP8-ΔmiR-M4, 1 ml (~10^6 $TCID_{50}$) of RCAS(A)-EGFP or RCAS(A)-v-*rel*-EGFP virus stock was used to infect $1x10^6$ of HP8-ΔmiR-M4 cells and HP8-Cas9 cells. EGFP expressing RCAS(A)-v-*rel*-EGFP and RCAS(A)- EGFP infected HP8-ΔmiR-M4 and HP8-Cas9 cells were sorted into 6 well plates. After 7 days incubation, cells were collected and examined for v-*rel*, EGFP expression by western blot and miR-155 expression by qRT-PCR.

Sorting

For single cell cloning, cells were washed twice with PBS containing 5% FBS and centrifuged at 450g for 5 min at room temperature. The cell pellets were resuspended in cold PBS/5%FBS and sorted into 96 well plate U bottom (Corning) with growth medium by FACS using FACSAria II (BD bioscience).

qRT-PCR analysis of miRNA expression

The expression level of miRNAs were analyzed using the TaqMan MicroRNA Assay System (Life Technologies) using 10 ng total RNA as a template for reverse transcription. Each reverse transcription reaction was tested by PCR in triplicate and performed twice independently. For relative quantification of miRNA-M4 in HP8-ΔmiR-M4 (Fig. 1d) and miR-155 in v-*rel* transduced cells (Fig. 5b), all values were normalized to the expression of the endogenous let-7a, and levels were calculated as fold-expression change relative to those from HP8-Cas9 cells (miR-155) and CEF (miR-M4). For relative quantification of viral miRNAs and host gga-let-7a in HP8-ΔmiR-M4 clone 48 and controls HP8-Cas9 and CEF (Fig.4a), all values were normalized to the expression of the endogenous GAPDH gene, and levels were calculated as fold-expression change relative to those from CEF.

Dual luciferase reporter assay

Previously constructed reporter construct for the validated miR-M4 and miR-155 target Pu.1 in psiCHECK vector was used to measure the miR-M4 activity in HP8 (28). The reporter constructs contain a 110-bp fragment of the chicken Pu.1 3′ untranslated region (UTR) sequence with MRE (Pu.1-3′UTR-wt) or MRE mutant sequence (Pu.1-3′UTR-mu) inserted downstream of Renilla luciferase in the psiCHECK-2 vector (Promega) (28). HP8-ΔmiR-M4 cells and HP8-Cas9 cells ($5x10^5$) were transfected with 4ug of either Pu.1-3′UTR-wt or Pu.1-3′UTR-mu using NEPA21 electroporator as described. The luciferase expression was assayed 48 h later using the Dual-Glo Luciferase Assay System (Promega) following the manufacturer's instructions. The relative expression of Renilla luciferase was determined with the normalized levels of firefly luciferase. For each sample, values from four replicates representative of at least two independent experiments were used in the analysis.

Western blotting analysis

Approximately 1x10^6 HP8-ΔmiR-M4 cells and the control cells were collected and boiled with TruPAGE^{TM} LDS sample buffer (Sigma) for 10 min. The samples were separated on a 4-12% TruPAGE^{TM} Precast Gel, and the resolved proteins were transferred onto PVDF membranes. Expression of Meq, Pu.1, v-*rel* and GFP was detected using anti-Meq monoclonal antibody (Mab) FD7 (21), rabbit anti-SPIB polyclonal antibody (Aviva Systems Biology), anti-v-*rel* Mab HY87 (35) and GFP Polyclonal Antibody (SICGEN) respectively. α-tubulin (Sigma Aldrich) was used as loading control in all cases. After probing with primary antibodies, the blots were incubated with secondary antibody IRDye®680RD goat anti-mouse IgG (LI-COR) (for Meq, v-*rel* and α-tubulin detection), IRDye®800CW Donkey anti-rabbit IgG (LI-COR) (for Pu.1 detection), IRDye®800CW Donkey anti-goat IgG (LI-COR) (for GFP detection) and visualized using Odyssey Clx (LI-COR). For GFP detection, the PVDF membrane used for v-*rel* detection was stripped and re-probed with GFP antibody following the same procedure.

Analysis of HP8-Cas9-ΔmiR-M4 cell growth

The growth of HP8-Cas9-ΔmiR-M4 clones along with non-edited HP8-Cas9 was monitored by IncuCyte S3 live cell imaging (Essen Bioscience Ltd, Hertfordshire, UK). Briefly, 8000 cells were seeded in a 96-well plate (Corning) and images were captured every 4h for 132h from four separate regions per well using a 10x objective. By recording the phase object confluence, the growth of HP8-Cas9-ΔmiR-M4 clones were compared with parental HP8-Cas9. IncuCyte data was analysed by two-way ANOVA with Tukey's multiple comparisons using GraphPad Prism version 7.01 (GraphPad Software, Inc., San Diego, CA). The results were shown as mean ± standard error (SE)

from four replicates each with 4 separate regions per well representative of three independent experiments. P values of < 0.05 were considered to be significant.

Acknowledgements: This project was supported by the Biotechnology and Biological Sciences Research Council (BBSRC) grants BBS/E/I/00007032, BB/R007632/1 and BB/R007896/1, PhD placement programme of UK-China Joint Research and Innovation Partnership Fund 201603780111, BBSRC Newton Fund Joint Centre Awards on "UK-China Centre of Excellence for Research on Avian Diseases", the National Natural Science Foundation of China grants (U1604232 & 31602050), Fund for Distinguished Young Scholars from Henan Academy of Agricultural Sciences (No. 2019JQ01). We thank Radmila Hrdlickova, Henry Bose Jr (University of Texas at Austin) and Tom Gilmore (Boston University) for kindly providing v-*rel* reagents.

Conflict of interest: The authors report no conflict of interest.

References

1. Cullen BR. 2006. Viruses and microRNAs. Nat Genet 38 Suppl:S25-30.
2. Skalsky RL, Cullen BR. 2010. Viruses, microRNAs, and host interactions. Annu Rev Microbiol 64:123-41.
3. Yao Y, Nair V. 2014. Role of virus-encoded microRNAs in Avian viral diseases. Viruses 6:1379-94.
4. Boss IW, Plaisance KB, Renne R. 2009. Role of virus-encoded microRNAs in herpesvirus biology. Trends Microbiol 17:544-53.
5. Parnas O, Corcoran DL, Cullen BR. 2014. Analysis of the mRNA targetome of microRNAs expressed by Marek's disease virus. MBio 5:e01060-13.
6. Zhao Y, Xu H, Yao Y, Smith LP, Kgosana L, Green J, Petherbridge L, Baigent SJ, Nair V. 2011. Critical role of the virus-encoded microRNA-155 ortholog in the induction of Marek's disease lymphomas. PLoS Pathog 7:e1001305.
7. Zhuang G, Sun A, Teng M, Luo J. 2017. A Tiny RNA that Packs a Big Punch: The Critical Role of a Viral miR-155 Ortholog in Lymphomagenesis in Marek's Disease. Front Microbiol 8:1169.
8. Eis PS, Tam W, Sun L, Chadburn A, Li Z, Gomez MF, Lund E, Dahlberg JE. 2005. Accumulation of miR-155 and BIC RNA in human B cell lymphomas. Proc Natl Acad Sci U S A 102:3627-32.
9. Kluiver J, Poppema S, de Jong D, Blokzijl T, Harms G, Jacobs S, Kroesen BJ, van den Berg A. 2005. BIC and miR-155 are highly expressed in Hodgkin, primary mediastinal and diffuse large B cell lymphomas. J Pathol 207:243-9.
10. van den Berg A, Kroesen BJ, Kooistra K, de Jong D, Briggs J, Blokzijl T, Jacobs S, Kluiver J, Diepstra A, Maggio E, Poppema S. 2003. High expression of B-cell receptor inducible gene BIC in all subtypes of Hodgkin lymphoma. Genes Chromosomes Cancer 37:20-8.
11. Tili E, Michaille JJ, Croce CM. 2013. MicroRNAs play a central role in molecular dysfunctions linking inflammation with cancer. Immunol Rev 253:167-84.
12. Linnstaedt SD, Gottwein E, Skalsky RL, Luftig MA, Cullen BR. 2010. Virally induced cellular microRNA miR-155 plays a key role in B-cell immortalization by Epstein-Barr virus. J Virol 84:11670-8.
13. Wood CD, Carvell T, Gunnell A, Ojeniyi OO, Osborne C, West MJ. 2018. Enhancer control of miR-155 expression in Epstein-Barr virus infected B cells. J Virol doi:10.1128/JVI.00716-18.
14. Gottwein E, Mukherjee N, Sachse C, Frenzel C, Majoros WH, Chi JT, Braich R, Manoharan M, Soutschek J, Ohler U, Cullen BR. 2007. A viral microRNA functions as an orthologue of cellular miR-155. Nature 450:1096-9.
15. Sin SH, Kim YB, Dittmer DP. 2013. Latency locus complements MicroRNA 155 deficiency in vivo. J Virol 87:11908-11.
16. Skalsky RL, Samols MA, Plaisance KB, Boss IW, Riva A, Lopez MC, Baker HV, Renne R. 2007. Kaposi's sarcoma-associated herpesvirus encodes an ortholog of miR-155. J Virol 81:12836-45.

17. Lee LF, Wu P, Sui D, Ren D, Kamil J, Kung HJ, Witter RL. 2000. The complete unique long sequence and the overall genomic organization of the GA strain of Marek's disease virus. Proc Natl Acad Sci U S A 97:6091-6.
18. Tulman ER, Afonso CL, Lu Z, Zsak L, Rock DL, Kutish GF. 2000. The genome of a very virulent Marek's disease virus. J Virol 74:7980-8.
19. Nair V, Kung HJ. 2004. Marek's disease virus oncogenicity: Molecular Mechanisms, p 32-48. *In* Davison F, Nair V (ed), Marek's Disease: An Evolving Problem, 1st ed. Elsevier Academic Press, London.
20. Parcells MS, Burnside J, Morgan RW. 2012. Marek's disease virus-induced T-cell lymphomas, p 307-335. *In* Robertson ES (ed), Cancer Associated Viruses. Springer.
21. Brown AC, Baigent SJ, Smith LP, Chattoo JP, Petherbridge LJ, Hawes P, Allday MJ, Nair V. 2006. Interaction of MEQ protein and C-terminal-binding protein is critical for induction of lymphomas by Marek's disease virus. Proc Natl Acad Sci U S A 103:1687-92.
22. Lupiani B, Lee LF, Cui X, Gimeno I, Anderson A, Morgan RW, Silva RF, Witter RL, Kung HJ, Reddy SM. 2004. Marek's disease virus-encoded Meq gene is involved in transformation of lymphocytes but is dispensable for replication. Proc Natl Acad Sci U S A 101:11815-20.
23. Petherbridge L, Brown AC, Baigent SJ, Howes K, Sacco MA, Osterrieder N, Nair VK. 2004. Oncogenicity of virulent Marek's disease virus cloned as bacterial artificial chromosomes. J Virol 78:13376-80.
24. Kaufer BB, Arndt S, Trapp S, Osterrieder N, Jarosinski KW. 2011. Herpesvirus telomerase RNA (vTR) with a mutated template sequence abrogates herpesvirus-induced lymphomagenesis. PLoS Pathog 7:e1002333.
25. Burnside J, Bernberg E, Anderson A, Lu C, Meyers BC, Green PJ, Jain N, Isaacs G, Morgan RW. 2006. Marek's disease virus encodes MicroRNAs that map to meq and the latency-associated transcript. J Virol 80:8778-86.
26. Morgan R, Anderson A, Bernberg E, Kamboj S, Huang E, Lagasse G, Isaacs G, Parcells M, Meyers BC, Green PJ, Burnside J. 2008. Sequence conservation and differential expression of Marek's disease virus microRNAs. J Virol 82:12213-20.
27. Yao Y, Zhao Y, Xu H, Smith LP, Lawrie CH, Watson M, Nair V. 2008. MicroRNA profile of Marek's disease virus-transformed T-cell line MSB-1: predominance of virus-encoded microRNAs. J Virol 82:4007-15.
28. Zhao Y, Yao Y, Xu H, Lambeth L, Smith LP, Kgosana L, Wang X, Nair V. 2009. A functional MicroRNA-155 ortholog encoded by the oncogenic Marek's disease virus. J Virol 83:489-92.
29. Yu ZH, Teng M, Sun AJ, Yu LL, Hu B, Qu LH, Ding K, Cheng XC, Liu JX, Cui ZZ, Zhang GP, Luo J. 2014. Virus-encoded miR-155 ortholog is an important potential regulator but not essential for the development of lymphomas induced by very virulent Marek's disease virus. Virology 448:55-64.
30. Mwangi WN, Smith LP, Baigent SJ, Beal RK, Nair V, Smith AL. 2011. Clonal structure of rapid-onset MDV-driven CD4+ lymphomas and responding CD8+ T cells. PLoS Pathog 7:e1001337.

31. Brown AC, Nair V, Allday MJ. 2012. Epigenetic regulation of the latency-associated region of Marek's disease virus in tumor-derived T-cell lines and primary lymphoma. J Virol 86:1683-95.
32. Mwangi WN, Vasoya D, Kgosana LB, Watson M, Nair V. 2017. Differentially expressed genes during spontaneous lytic switch of Marek's disease virus in lymphoblastoid cell lines determined by global gene expression profiling. J Gen Virol 98:779-790.
33. Zhang Y, Tang N, Sadigh Y, Baigent S, Shen Z, Nair V, Yao Y. 2018. Application of CRISPR/Cas9 Gene Editing System on MDV-1 Genome for the Study of Gene Function. Viruses 10.
34. Yao Y, Zhao Y, Smith LP, Lawrie CH, Saunders NJ, Watson M, Nair V. 2009. Differential expression of microRNAs in Marek's disease virus-transformed T-lymphoma cell lines. J Gen Virol 90:1551-9.
35. Yao Y, Vasoya D, Kgosana L, Smith LP, Gao Y, Wang X, Watson M, Nair V. 2017. Activation of gga-miR-155 by reticuloendotheliosis virus T strain and its contribution to transformation. J Gen Virol 98:810-820.
36. Grundhoff A, Sullivan CS. 2011. Virus-encoded microRNAs. Virology 411:325-43.
37. Kincaid RP, Sullivan CS. 2012. Virus-encoded microRNAs: an overview and a look to the future. PLoS Pathog 8:e1003018.
38. Morgan RW, Burnside J. 2011. Roles of avian herpesvirus microRNAs in infection, latency, and oncogenesis. Biochim Biophys Acta 1809:654-9.
39. Yao Y, Bassett A, Nair V. 2016. Targeted editing of avian herpesvirus vaccine vector using
CRISPR/Cas9 nucleases. Journal of Vaccine and Technologies 1.
40. Akiyama Y, Kato S. 1974. Two cell lines from lymphomas of Marek's disease. Biken J 17:105-16.
41. Zhang Y, Luo J, Tang N, Teng M, Reddy V, Moffat K, Shen Z, Nair V, Yao Y. 2019. Targeted Editing of the pp38 Gene in Marek's Disease Virus-Transformed Cell Lines Using CRISPR/Cas9 System. Viruses 11.

Figure legends

Figure 1. Deletion of the miR-M4 by CRISPR/Cas9 editing in HP8 cells. (a) The nucleic acid sequences of the truncated/edited PCR products showing the successful deletion of miR-M4 on selected clones. Target sequence is underlined, PAM sequence is in light blue and the cleavage site is indicated by an arrow. (b) The predicated stem loop structure of the pre-miR-M4 with the predicated cleavage site indicated by an arrow. The sequence of the mature miRNA sequences are shown in red. (c) PCR amplification of the

edited region using primers NF and CR on the cell lysates of transfected cells at 2 days post transfection and on isolated single cell clones C7-C11. (d) Relative expression of miR-M4, measured by qRT-PCR in RNA extracted from miR-M4 deleted clones C7, C37, C40, and C48 along with the un-edited HP8-Cas9 and CEF. The level of miR-M4 in HP8-Cas9 was set as 1 for calibration.

Figure 2. Proliferation of the HP8-Cas9 and the miR-M4 deleted clones monitored in real time using IncuCyte S3 live imaging system. Cell phase object confluence of each cell population was determined every 4h for 132h from 4 separate regions per well and 4 wells per sample in 96-well plate by IncuCyte and compared with HP8-Cas9 control. Growth curves are shown as mean ± standard error (SE) representative of three independent experiments. Asterisk (*) indicates statistically significant differences between miR-M4 deleted clones and parental HP8-Cas9 cells at different times. *, $p<0.05$; **, $p<0.01$; ***, $p<0.001$; ****, $p <0.0001$. Asterisks were placed above the time points (single time points) or underneath the growth curves for those time points with the same results during the indicated period of time.

Figure 3. Successful deletion of miR-M4 measured by functional studies. (a) Firefly and Renilla luciferase activities were measured consecutively with the dual luciferase reporter system (Promega) following transfection of reporter constructs containing the wild-type or the mutant MRE region of the 3′ UTR of miR-M4 target gene Pu.1 into the miR-M4 deleted cells and the parental HP8-Cas9. The relative expression of Renilla luciferase was determined with the normalized levels of firefly luciferase. For each sample, values from four replicates representative of at least two independent experiments were used in the analysis. The value from the psiCHECK-2-mutant was set

as 1. Error bars are derived from four replicates. (b) IP-western blot analysis of Pu.1 in miR-M4 deleted HP8 clone C48 and HP8-Cas9. Matched inputs were assayed for α-tubulin as loading control. Relative signal intensities of the Pu.1 Western blot band were quantified using ImageQuant and normalized against the corresponding signal from the tubulin band. The signal from HP8-Cas9 cells was set as 1.

Figure 4. MDV miRNAs and Meq protein expression in miR-M4 deleted cells. (a) Relative expression of each indicated viral miRNAs and host miRNA let-7a is measured by qRT-PCR with RNA extracted from miR-M4 deleted clone C48 along with the un-edited HP8-Cas9 and CEF. All values were normalized to the expression of the endogenous GAPDH gene, and levels were calculated as fold-expression change relative to those from CEF. The level of each miRNA in HP8-Cs9 was set as 1. (b) Detection of Meq expression by western blotting with anti-Meq monoclonal antibody FD7 in HP8-Cas9 and HP8-Cas9-ΔmiR-M4 clones. ALV transformed B-cell line HP45 and un-infected CEF were included as negative controls. For the loading control, the same blot was stripped and reprobed with anti-α-tubulin antibody.

Figure 5. Upregulation of miR-155 in miR-M4 deleted HP8 by v-*rel*. (a) Detection of v-*rel* expression with anti-v-*rel* monoclonal antibody HY87 and GFP expression with anti-GFP antibody by western blotting in HP8-ΔmiR-M4 clone C48 and HP8-Cas9 infected with RCAS(A)-GFP or RCAS(A)-v-*rel*-GFP respectively. For the loading control, the same blot was stripped and reprobed with anti-α-tubulin antibody. (b) Relative level of miR-155 expression was detected by qRT-PCR in HP8-ΔmiR-M4 clone C48 and HP8-Cas9 infected with RCAS(A)-GFP or RCAS(A)-v-*rel*-GFP respectively.

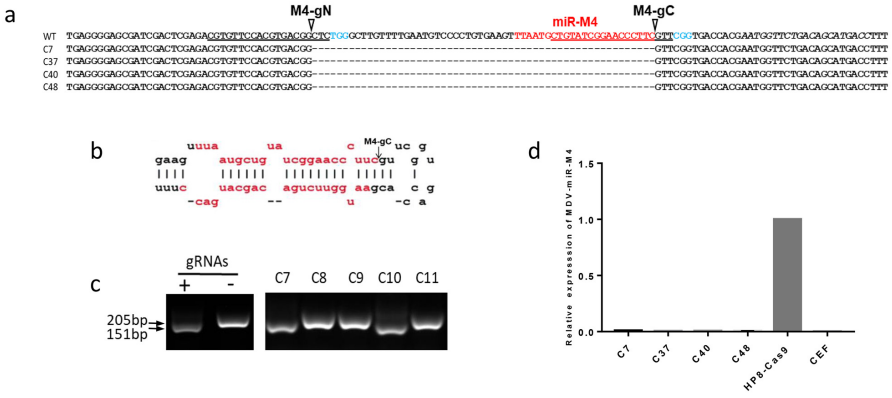

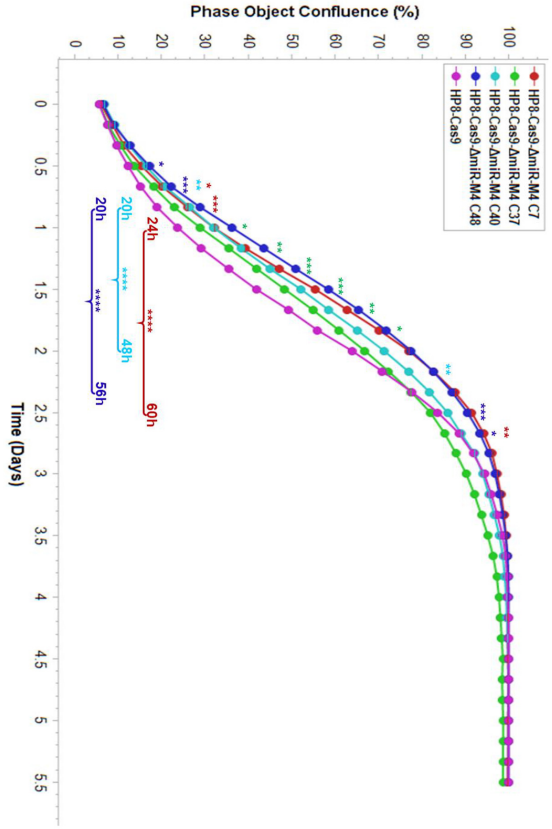

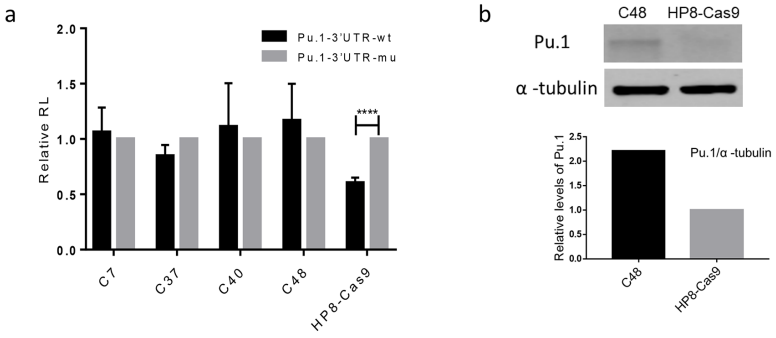

a

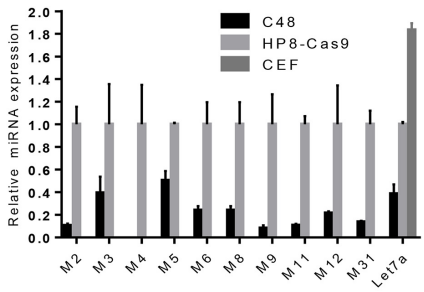

b

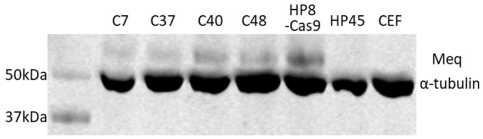

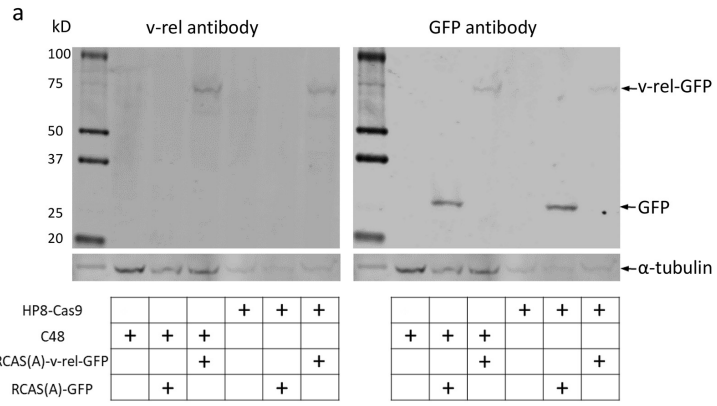

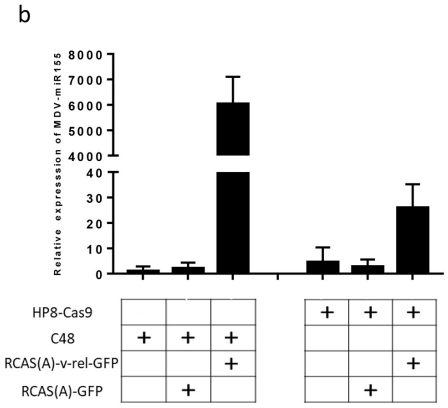

Table 1. List of primer sequences

Primer	Sequence (5'-3')
miR-M4-gN	CGTGTTCCACGTGACGGCTC
miR-M4-gC	CTGTATCGGAACCCTTCGTT
miR-M4-F	TGAGGGGAGCGATCGACTC
miR-M4-R	GATTCAATATTACATCACTTCAACGG